

1 **Full Title: Impact of extrinsic incubation temperature on natural selection during Zika
2 virus infection of *Aedes aegypti*.**

3 **Short Title: Temperature impacts on Zika virus population structure**

4 Authors: Reyes A. Murrieta¹, Selene Garcia-Luna^{1,2}, Deedra J. Murrieta¹, Gareth Halladay¹,
5 Michael C. Young¹, Joseph R. Fauver^{1,3}, Alex Gendernalik¹, James Weger-Lucarelli^{1,4}, Claudia
6 Rückert^{1,5}, Gregory D. Ebel^{1*}

7

8 **Affiliations:**

9 ¹Department of Microbiology, Immunology and Pathology, College of Veterinary Medicine and
10 Biomedical Sciences, Colorado State University, Fort Collins, CO 80523, USA

11 ²Department of Entomology, Texas A&M University, College Station, TX 77840, USA

12 ³Yale School of Public Health, Department of Epidemiology of Microbial Diseases, Laboratory of
13 Epidemiology of Public Health, New Haven, CT 06510, USA

14 ⁴Department of Biomedical Sciences & Pathobiology, Virginia-Maryland College of Veterinary
15 Medicine, Virginia Tech, Blacksburg, VA 24061, USA

16 ⁵Department of Biochemistry and Molecular Biology, College of Agriculture, Biotechnology &
17 Natural Resources, University of Nevada, Reno, NV 89557, USA

18 *Corresponding author: Gregory D. Ebel

19 E-mail: gregory.ebel@colostate.edu

20

21

23 **Abstract**

24 Arthropod-borne viruses (arboviruses) require replication across a wide range of temperatures
25 to perpetuate. While vertebrate hosts tend to maintain temperatures of approximately 37°C -
26 40°C, arthropods are subject to ambient temperatures which can have a daily fluctuation of >
27 10°C. Temperatures impact vector competence, extrinsic incubation period, and mosquito
28 survival unimodally, with optimum occurring at some intermediate temperature. In addition, the
29 mean and range of daily temperature fluctuations influence arbovirus perpetuation and vector
30 competence. The impact of temperature on arbovirus genetic diversity during systemic mosquito
31 infection, however, is poorly understood. Therefore, we determined how constant extrinsic
32 incubation temperatures of 25°C, 28°C, 32°C, and 35°C control Zika virus (ZIKV) vector
33 competence and population dynamics within *Aedes aegypti* and *Aedes albopictus* mosquitoes.
34 We also examined diurnally fluctuating temperatures which more faithfully mimic field conditions
35 in the tropics. We found that vector competence varied in a unimodal manner for constant
36 temperatures peaking between 28°C and 32°C for both *Aedes* species. Transmission peaked at
37 10 days post-infection for *Aedes aegypti* and 14 days for *Aedes albopictus*. The effect of diurnal
38 temperature was distinct and could not have been predicted from constant temperature-derived
39 data. Using RNA-seq to characterize ZIKV population structure, we identified that temperature
40 alters the selective environment in unexpected ways. During mosquito infection, constant
41 temperatures more often elicited positive selection whereas diurnal temperatures led to strong
42 purifying selection in both *Aedes* species. These findings demonstrate that temperature has
43 multiple impacts on ZIKV biology within mosquitoes, including major effects on the selective
44 environment within mosquitoes.

45

46

47 **Author Summary**

48 Arthropod-borne viruses (arboviruses) have emerged in recent decades due to complex factors
49 that include increases in international travel and trade, the breakdown of public health
50 infrastructure, land use changes, and many other factors. Climate change also has the potential
51 to shift the geographical ranges of arthropod vectors, consequently increasing the global risk of
52 arbovirus infection. Changing temperatures may also alter the virus-host interaction, ultimately
53 resulting in the emergence of new viruses and virus genotypes in new areas. Therefore, we
54 sought to characterize how temperature (both constant and fluctuating) alters the ability of
55 *Aedes aegypti* and *Aedes albopictus* to transmit Zika virus, and how it influences virus
56 populations within mosquitoes. We found that intermediate temperatures maximize virus
57 transmission compared to more extreme and fluctuating temperatures. Constant temperatures
58 increased positive selection on virus genomes, while fluctuating temperatures strengthened
59 purifying selection. Our studies provide evidence that in addition to altering VC, temperature
60 significantly influences the selective environment within mosquitoes.

61

62

63

64

65

66

67

68

69 **Introduction**

70 Arthropod-borne viruses (arboviruses) such as Zika virus (ZIKV, Flaviviridae, *Flavivirus*) are
71 mainly RNA viruses that are transmitted by arthropod vectors among vertebrate hosts [1]. Thus,
72 arboviruses are required to alternately replicate in hosts with drastically different body
73 temperatures. This affects transmission dynamics, replication rates, and population structure.
74 While replication in vertebrates generally occurs within 2-3 degrees of 38°C [2], infection in
75 mosquitoes may occur at a much wider range of temperatures: Mosquito vectors are distributed
76 throughout tropical and temperate climates and the geographical range of important species is
77 increasing [3]. Climate variations such as heat waves, cold snaps, or daily temperature
78 fluctuations change the host environment within which arboviruses replicate and are
79 transmitted. Fluctuations in the temperature of the host environment are central to arbovirus
80 biology [4] and virus-host interaction [5-7].

81 The impact of temperature on vector competence (VC), i.e. the ability of a mosquito to acquire,
82 maintain, and transmit a pathogen, is well described. Temperature increases impact VC in a
83 unimodal manner (having one clear peak), with extreme low (16°C) and high (38°C)
84 temperatures having low VC while median temperatures (28°C -32°C) have higher VC [8, 9].
85 The extrinsic incubation temperature (EIT) also influences viral replication and dissemination
86 within vectors [10-15], altering the extrinsic incubation period, i.e. the number of days between
87 acquisition of an infection and infectiousness to a new host [5, 16]. Most studies examining the
88 effects of temperature on VC have used single, constant temperatures to represent optimal
89 conditions for mosquito colony survival [17-20]. However, diurnal temperature fluctuations more
90 accurately model the environmental conditions encountered by mosquitoes in the field [21-24].
91 Although temperature clearly exerts a strong selective pressure on RNA viruses [25, 26], little is
92 known about how it may influence the composition of arbovirus populations during mosquito

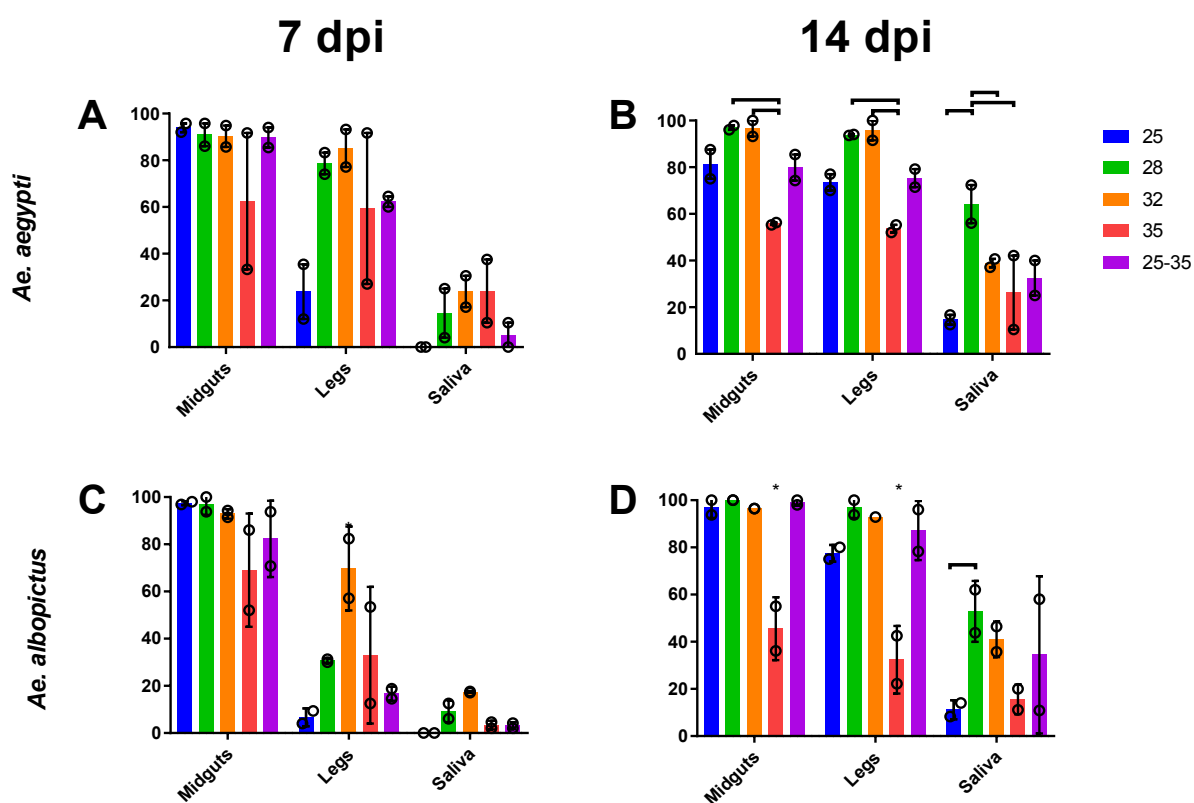
93 infection. Thus, while temperature clearly effects arbovirus transmission and epidemiology, its
94 impact on arbovirus evolution remains unclear.

95 RNA viruses like ZIKV have the capacity to evolve rapidly in response to changing
96 environments. This is due, in part, to short generation times and error-prone replication [27, 28].
97 As a result, arboviruses, including ZIKV, exist within hosts as large populations of mixed
98 haplotypes, which is critical to their perpetuation in nature [29-33]. While there have been
99 numerous studies assessing ZIKV VC and viral ecology and some efforts focusing on the use of
100 environmental data to predict virus spread, there is limited knowledge as to how environmental
101 factors such as temperature impact the selective environments and mutational diversity of
102 arboviruses within mosquitoes. Accordingly, we sought to determine whether ZIKV mutational
103 diversity is altered by EIT during systemic infection of *Ae. aegypti* and *Aedes albopictus* (*Ae.*
104 *albopictus*) vectors. We exposed mosquitoes to a Puerto Rican isolate of ZIKV and held them at
105 constant temperatures of 25°C, 28°C, 32°C, 35°C; and a diurnal fluctuation from 25°C to 35°C.
106 We then assessed VC and measured virus mutational diversity in different tissue compartments
107 of each mosquito using next-generation sequencing (NGS). Our results suggest that the
108 selective environment within mosquitoes is significantly modified by temperature, and that
109 temperature fluctuations exert unique constraints upon arbovirus sequences.

110 **Results**

111 To assess how extrinsic incubation temperature affects vector competence for ZIKV we
112 exposed *Ae. aegypti* and *Ae. albopictus* to ZIKV (n=72-108), held them at 25°C, 28°C, 32°C,
113 35°C, and alternating diurnal temperature that fluctuated between 25°C-35°C. Infection rates
114 were high in all mosquitoes except those held at 35°C (Fig 1). In both *Aedes* species, moderate
115 temperatures (28°C and 32°C) significantly ($p < 0.05$, Two-tailed Fisher's exact test) increased
116 dissemination and transmission at 7 days post-infection (Fig 1A & 1C). The difference in
117 dissemination was most notable in *Ae. albopictus*, which was ~30% at 28°C and ~80% at 32°C

118 (Fig 1A). Our diurnal temperature group did not fit with the expected unimodal distribution given
119 the mean daily temperature in this group (30°C). Instead, infection in this temperature group
120 was lower, and most closely resemble infection rates of the 25°C and 28°C temperatures or
121 32°C and 35°C temperatures. Mosquitoes experiencing diurnal temperatures also had
122 significantly lower dissemination and transmission ($p < 0.05$, Two-tailed Fisher's exact test)
123 compared to the standard laboratory colony temperature of 28°C, which is used for most VC
124 studies. [diurnal temperature depressed aedes vector competence compared to the optimal,
125 mean temperature.]

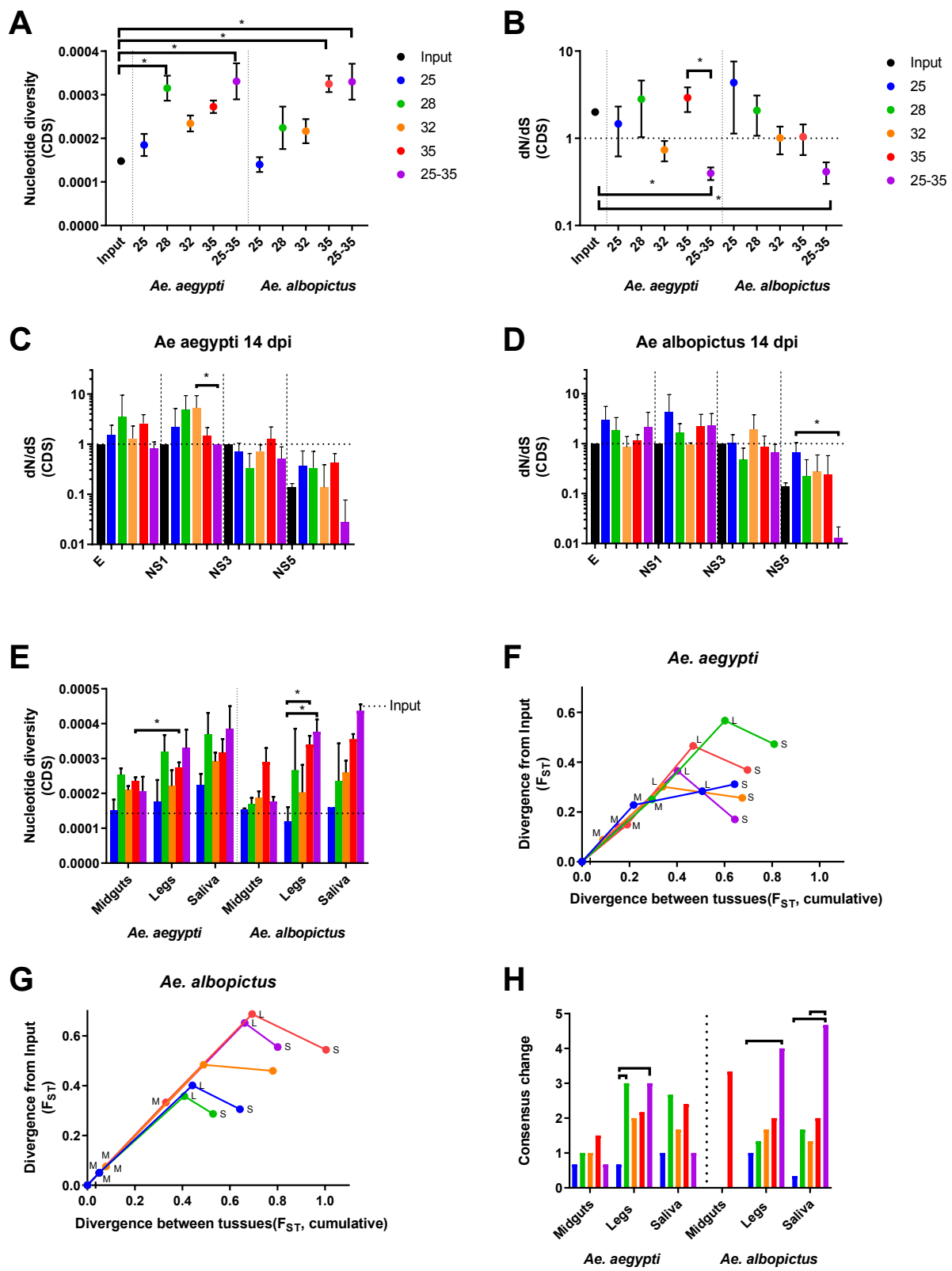


126

127 **Fig 1. Extrinsic incubation temperature alters ZIKV transmission efficiency in Aedes**
128 **mosquitoes.** Percent of Ae. aegypti (A & B) and Ae. albopictus (C & D) with ZIKV in midgut,
129 legs, and saliva at 7 (A & C) and 14 (B&D) days post feeding. The bar represents the mean and
130 the open circles represent the value of each experiment with SEM shown with error bars.

131 Brackets above vertical bars indicate statistical significance between indicated groups, asterisks
132 indicate significance from the entire species-tissue group ($p < 0.05$, Two-tailed Fisher's exact
133 test).

134 Consensus-level changes were rarely observed in ZIKV in these experiments. We therefore
135 assessed the effect of temperature and mosquito species on ZIKV mutational diversity at the
136 intrahost level by sequencing virus collected from 3 biological replicates of tissues (midgut, legs,
137 and saliva) harvested from *Ae. aegypti* and *Ae. albopictus* at 14 days post exposure. Nucleotide
138 diversity across the coding sequence was lowest in mosquitoes held at 25°C and highest in
139 mosquitoes held at 35°C or under a diurnally fluctuating temperature regime. Minimal
140 differences were observed when comparing *Ae. aegypti* to *Ae. albopictus* (Fig 2A). d_N/d_S was
141 estimated across the coding sequence to assess selection acting upon viral genomes. In both
142 *Aedes* species, d_N/d_S was significantly lower in ZIKV from diurnal-exposed mosquitoes
143 compared to those held at constant temperatures, and solely virus from these mosquitoes had
144 d_N/d_S much lower than 1 (Fig 2B). Similar levels of richness, complexity, and divergence were
145 observed in all mosquitoes and EIT groups (Not Shown).



147 **Fig 2. Temperature alters virus diversification, selection and divergence during mosquito**
148 **infection.** ZIKV population diversity at varying temperatures was determined using measures of
149 nucleotide diversity (A) and natural selection (d_N/d_S) (B). d_N/d_S was also examined by virus
150 coding region for virus that replicated in *Ae. aegypti* (C), and *Ae. albopictus* (D). Results for E,
151 NS1, NS3, and NS5 protein coding regions are shown. d_N/d_S was near 1 for C, prM NS2A,
152 NS2B, NS4A, NS4B (not shown. Nucleotide diversity (E) and divergence (F-G) were determined
153 for ZIKV in different mosquito compartments. Divergence from input population (y-axis) and
154 cumulative divergence between tissues (x-axis) (F-G) is presented. Midguts (M), legs (L), Saliva
155 (S). Consensus change counts also are presented (H) by temperature and mosquito species.,
156 and majority variants accumulated (H), as markers of population diversity. Significance was
157 tested using the Kruskal-Wallis test with Dunn's correction (A-D, H, * p < 0.05) or 2-way ANOVA
158 with Tukey's (E, p-value < 0.05). Figures present the mean and SEM (A-B, E) or 95% CI (C-D).

159 To assess coding region-specific signatures of selection, we analyzed d_N/d_S for each viral
160 protein coding sequence independently. In both mosquito species exposed to diurnal
161 temperatures, d_N/d_S was much less than 0.1 only within the NS5 coding sequence (Fig 2C-D
162 mean d_N/d_S 0.027 in *Ae. aegypti* and 0.0132 in *Ae. albopictus*). E and NS1 coding sequences
163 had d_N/d_S greater than 1 when temperatures were constant, ranging from a mean d_N/d_S of 1.298
164 at 32°C in E to 5.325 at 32°C in NS1 in *Ae. aegypti*. *Ae. albopictus* had a mean low d_N/d_S of
165 1.154 at 35°C in E and a high of 4.267 at 25°C in NS1, the exception being 32°C in *Ae.*
166 *albopictus* where d_N/d_S was 0.0853 (E) and 0.9804 (NS1) respectively (Fig 2C-D).

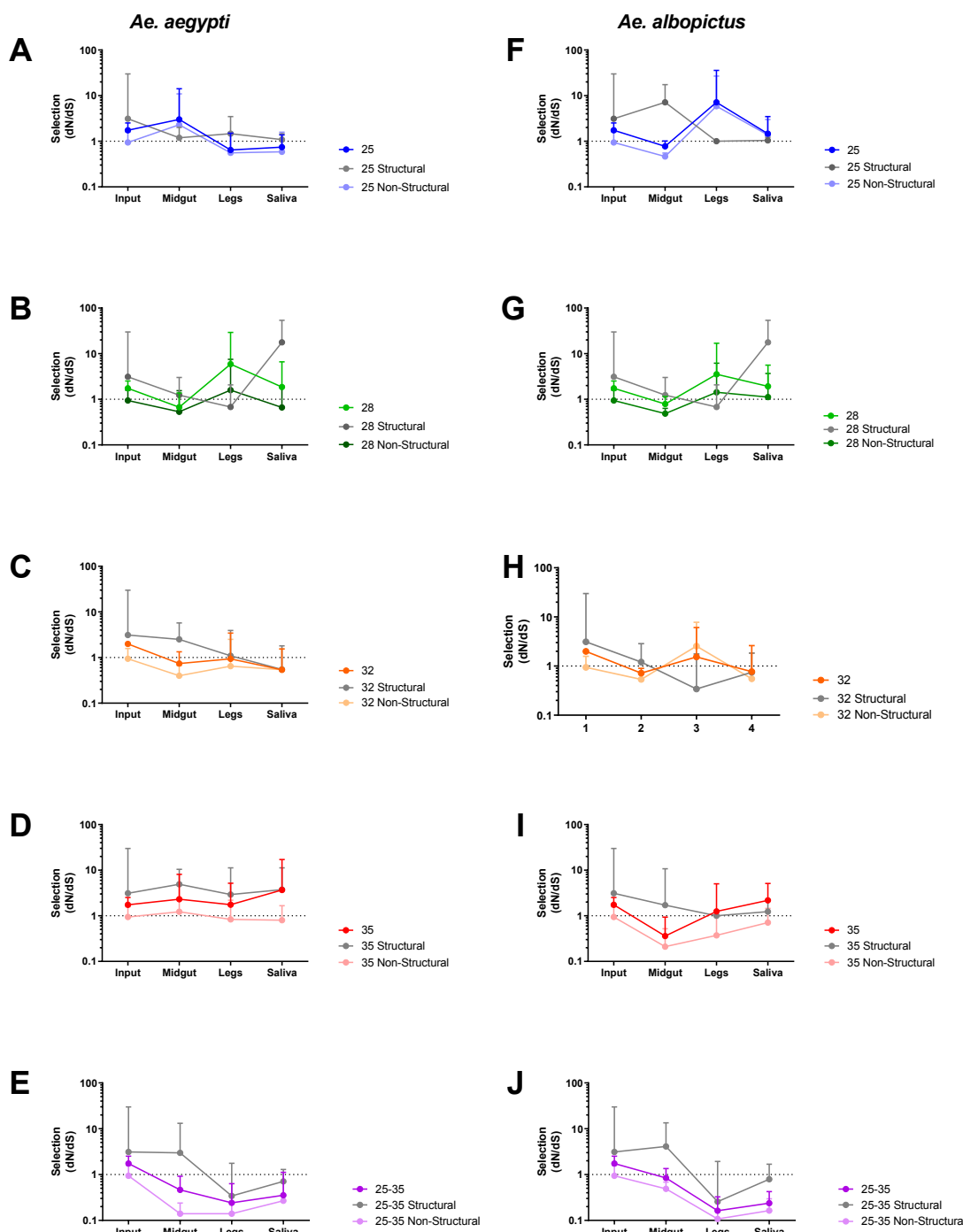
167 Since arboviruses encounter multiple replication environments and barriers during systemic
168 mosquito infection, we next assessed intrahost population diversity in the midguts, legs, and
169 saliva of mosquitoes held at varying temperatures (Fig 2E-H). In all tissue compartments of both
170 species tested, nucleotide diversity tended to increase with increasing temperature (Fig 2E),
171 with diurnally-exposed mosquitoes having lower diversity during midgut infection but increased

172 genetic diversity during systemic infection that resulted in some of the highest levels of
173 nucleotide diversity in leg and saliva-associated virus (Fig 2E). Analysis of the fixation index
174 (F_{ST}), during systemic infection revealed temperature- and species-specific patterns of
175 divergence from the input population (Fig 2F-G). Generally, ZIKV diverged more in the midguts
176 of *Ae. aegypti* than *Ae. albopictus*. The 28°C EIT group diverged more than any other EIT group
177 in *Ae. aegypti* (Fig 2F). Whereas in *Ae. albopictus*, exposure to higher temperatures of 32°C
178 and 35°C promote divergence. In both species, divergence was greatest when the population
179 disseminated from the midgut to the legs and decreased from legs to saliva. These data provide
180 evidence that divergence from the founding population was increased in the midgut and legs of
181 both species and reduced as virus moved from legs to saliva, potentially due to stochastic
182 reductions caused by bottlenecks and/or purifying selection.

183 Patterns of ZIKV population diversity during systemic infection are temperature dependent. This
184 also is reflected in the number of changes to the consensus virus sequence (Fig 2H). Increasing
185 temperature tended to increase the number of consensus changes, with 28°C somewhat of an
186 outlier. Significantly more consensus changes were observed in *Ae. albopictus* for diurnal
187 temperatures than any constant temperature group (Fig 2H).

188 Since ZIKV population diversity is influenced by the tissues of origin, as well as the constant and
189 diurnal EIT, we assessed d_N/d_S during systemic infection for each EIT group across the entire
190 CDS, and for the structural and nonstructural regions independently (Fig 3). Our input
191 population had a d_N/d_S ratio of 1.75 for the CDS, 3.11 for the structural region, and 0.95 for the
192 non-structural regions. This indicates that the structural regions of our input population were
193 under positive selection (d_N/d_S greater than 1) during its propagation and preparation, whereas
194 the non-structural regions were not. Interestingly, when ZIKV was exposed to diurnal fluctuating
195 temperatures, it was under strong purifying selection (d_N/d_S less than 1) in both *Aedes* species
196 (Fig 3E & 3J), whereas all constant temperatures caused ZIKV d_N/d_S generally near or above 1

197 (Fig 3). In the saliva, 25°C and 32°C EIT groups had a d_N/d_S that neared 1, decreasing from the
 198 input in both *Aedes* species (Fig 3A, 3C, 3F, 3H). Conversely, 28°C and 35°C EIT groups
 199 maintained or increased d_N/d_S when compared to input (Fig 3B, 3D, 3G, 3I).



200

201 **Fig 3. Fluctuating diurnal temperatures impose purifying selection on ZIKV during**
202 **systemic mosquito infection.** d_N/d_S (mean with 95% CI) for ZIKV CDS (closed circles),
203 structural sequence (Boxes). And Non-structural sequence (open circles), at indicated
204 temperatures, including diurnal fluctuating temperatures, in *Ae. aegypti* (A-E) and *Ae. albopictus*
205 (F-J).

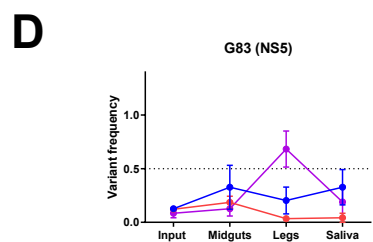
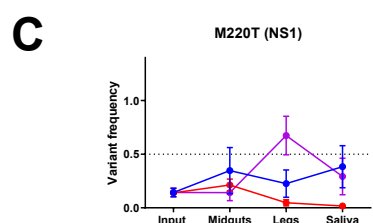
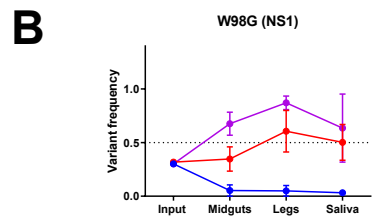
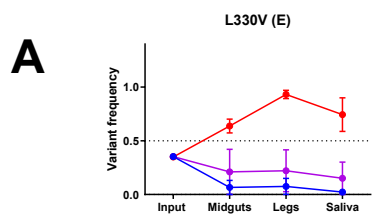
206 Although relatively few consensus level changes occurred in ZIKV after replication in
207 mosquitoes, we identified a handful of changes to the ZIKV genome that occurred
208 independently in several mosquito tissues (Table 1). Of these consensus changes, 3
209 nonsynonymous and 1 synonymous SNVs were found in both *Ae. aegypti* and *Ae. albopictus*
210 (L330V E, W98G NS1, M220T NS1, and G83 NS5) samples. The remaining 4 consensus
211 changes were comprised of 1 non-synonymous mutation (T315I E) unique to *Ae. aegypti* and 3
212 mutations unique to *Ae. albopictus*: 1 non-synonymous mutation and 2 synonymous mutations
213 (K146E NS1, I94 NS2A and F682 NS5). All were present as minority variants in the input virus
214 population, and several have been documented in ZIKV genomic epidemiologic studies. (Table
215 1). These consensus changes tended to rise or fall in frequency in a species- and temperature-
216 dependent manner (Figure 4). In general, high and/or diurnal temperature tended to drive
217 variants to higher frequency in the population, while at the low temperature (25°C) variants
218 tended to remain closer to their input frequency. The frequency of the synonymous variant G83
219 in NS5 fluctuated in frequency similarly to M220T, suggesting linkage on the viral genome.

Species	Coding Sequence	AA	Input Freq ^a	Freq found ^b in Nature	Temperature Obs. ^c	Tissue ^d Obs.
<i>Aedes spp.</i>	E	L330V	0.35	100%	28, 32, 35, 25-35	M, L, S
	NS1	W98G	0.30	0%	28, 32, 35, 25-35	M, L, S
	NS1	M220T	0.14	0%	25, 28, 32, 35, 25-35	M, L, S
	NS5	G83	0.13	0%	25, 28, 32, 35, 25-35	M, L, S
<i>Ae. aegypti</i>	E	T315I	0.05	0%	28, 35	M, L, S
<i>Ae. albopictus</i>	NS1	K146E	0.01	2%	25, 28, 32, 25-35	L, S
	NS2A	I94	0.03	0.7%	35, 25-35	M, L, S
	NS5	F682	0.03	0%	35, 25-35	M, L, S

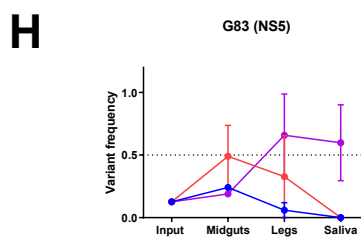
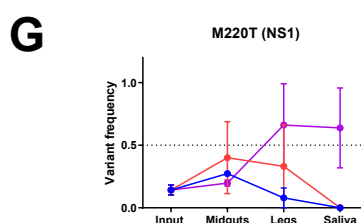
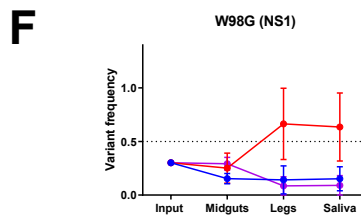
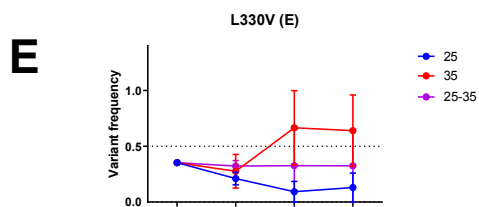
220

221 **Table 1. Multiple ZIKV variants found in across biological samples and temperatures go**
222 **to consensus.** ^a Variant frequency found in the stock input ZIKV population. ^b The percent
223 sequence identity observed in nature when aligned to 150 complete ZIKV genomes. ^c Extrinsic
224 incubation temperatures at which each variant was observed, ^d and tissues that each variant
225 was observed. Black= both species, Blue= Ae. aegypti only, Red= Ae. albopictus only. M,
226 midguts; L, legs; S, saliva.

Ae. aegypti



Ae. albopictus



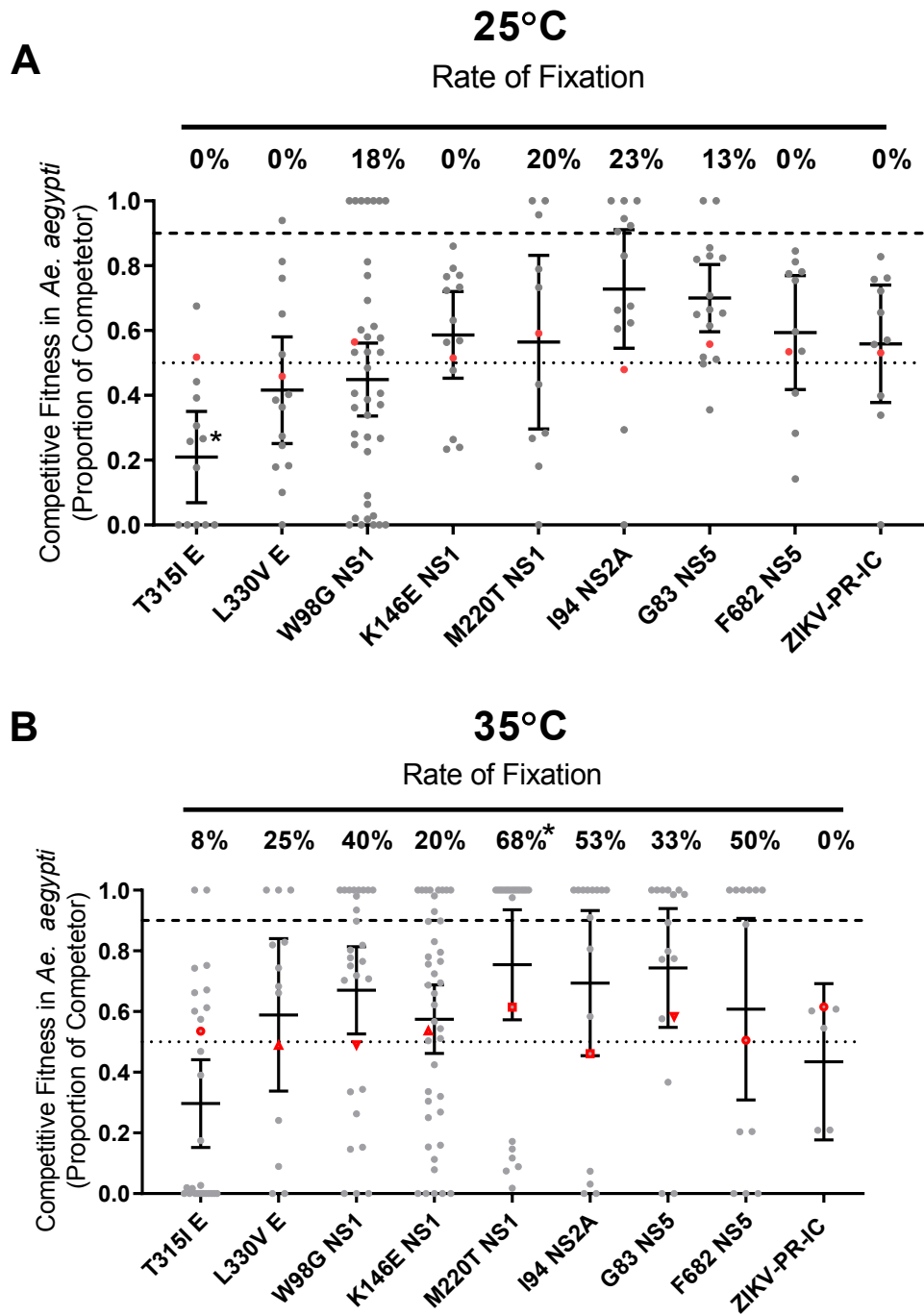
227

228 **Fig 4. EIT and species control ZIKV variant frequency during systemic infection.**

229 Frequencies of L330V E (A & E), W98G NS1 (B & F), M220T NS1 (C & G), and G83 NS5 (D &
230 H) in input, midgut, legs and saliva shown at 25, 35 and diurnal 25-35C in *Ae. aegypti* (A-D) and

231 Ae. *albopictus* (E-H). Mean and SEM of competitions from three biological replicates shown. We
232 then competed engineered ZIKV mutants containing the eight consensus-changing mutations
233 that arose during systemic infection (Table 1) in mosquitoes under low (25°C) and high (35°C)
234 EITs (Figure 5) to assess whether the fitness of these variants may be temperature-
235 dependent. Control competitions with marked and unmarked clones of the PRVABC59 virus
236 were unremarkable, with no significant changes in test to reference virus detected at either EIT.

237 Several mutants tended to rise in frequency at both 25°C and 35°C, with the overall rate of
238 fixation (mutants that reached 100% frequency as measured by our assay) higher in
239 mosquitoes held at 35°C ($p<0.001$, Two-tailed Fisher's exact test). The fitness implications of
240 these mutants tended to be variable. For example, in orally exposed Ae. *aegypti* bodies, the
241 clone bearing the NS1 M220T mutant had a significant ($p<0.05$, Kruskal-Wallis and Dunn's)
242 fitness advantage 14 days after blood feeding compared to wildtype. Conversely, the
243 envelope T315I mutant had significantly decreased ($p<0.05$, Kruskal-Wallis and Dunn's)
244 fitness compared to ZIKV-PR-IC at 25°C.



245

246 **Fig 5. High temperature increases variant fixation in *Aedes aegypti*.**

247 Indicated mutations were engineered into a ZIKV-PR-IC and mixed with a ZIKV-REF virus. The
248 proportion of each competitor (grey, mean with 95% CI, *p-value < 0.05 compared with ZIKV-

249 PR-IC , Kruskal-Wallis and Dunn's) and rate of fixation (*p-value < 0.05 compared with ZIKV-
250 PR-IC , Two-tailed Fisher's exact test) was determined from mosquito bodies at 14-dpi for *Ae.*
251 *aegypti* mosquitoes held at constant EIT's 25°C (A) & 35°C (B). Fixation indicate that 100% of
252 the sequenced nucleotides were from the competitor virus. Initial viral inoculum (ratio of
253 competitor virus to reference) is shown in red symbols.

254 **Discussion**

255 **Extrinsic incubation temperature alters vector competence**

256 Vector competence is largely determined by barriers to infection and escape from mosquito
257 midgut and salivary glands [4, 34]. Our results support the extensive existing literature [8, 9, 35]
258 that EIT controls infection and escape mechanisms, resulting in a unimodal distribution of VC
259 values: Extreme low 25°C and high 35°C temperatures had the lowest VC, while moderate
260 temperatures of 28°C and 32°C had peak VC (Fig 1). These results agree with previous
261 studies [8] and mechanistic models predicting the ZIKV thermal optimal limit of 29°C for *Ae.*
262 *aegypti* [8, 36]. However, the VC of mosquitoes held at diurnal temperatures were
263 consistently lower than the moderate temperatures of 28°C and 32°C despite having a similar
264 mean temperature. The reasons for this are unlikely caused by direct effects of temperature
265 on virus replication because ZIKV readily undergoes replication in vertebrates that commonly
266 maintain temperatures of 37°C, higher than any temperature tested here. It seems more
267 likely that the depressed VC observed at higher temps is due to indirect alterations to some
268 aspect of the mosquito environment caused by thermal stress. While our study does not
269 capture behavioral and physiological adaptations of mosquitoes to high temperatures, our
270 data clearly demonstrate that rapidly fluctuating temperatures negatively influence mosquito
271 vector competence for ZIKV compared to optimal constant temperatures.

272 **Temperature and vector species alter the selective environment within mosquitoes.**

273 Our data on intrahost population structure during systemic infection provides several novel
274 insights into how temperature alters the selective environment in epidemiologically relevant
275 arbovirus vectors. First, our data demonstrate that, in general, increasing temperature leads to
276 increases in nucleotide diversity (Fig 2A). This may simply reflect faster virus replication at
277 higher temperatures, with additional rounds of replication introducing additional mutations in a
278 somewhat clocklike fashion. Alternatively, it may be that this increase in nucleotide diversity
279 reflects the strength of positive selection at higher temperatures. The exception to this is
280 mosquitoes that were held at 28°C. While we cannot currently explain the higher diversity in
281 virus from these mosquitoes, it is notable that our colony has been maintained at 28°C for more
282 than 25 generations. Mosquitoes held at diurnally fluctuating temperatures, as above, were
283 somewhat atypical in that they tended to have higher levels of nucleotide diversity than one
284 would expect given the distribution of diversity observed in mosquitoes held at constant
285 temperature. As in the case of VC, diurnal temperature fluctuations are distinct in their impacts
286 on virus-host interactions when compared to constant temperatures and thus the impact and
287 strength of selection is also distinct.

288 Analysis of synonymous and nonsynonymous variation at the intrahost level revealed that
289 signatures of strong purifying selection were observed only in mosquitoes held at diurnal
290 temperatures (Fig 2B-D; Fig 3E, J). This observation provides an important counterpoint to
291 several previous studies that have documented a relaxation of purifying selection in flaviviruses
292 that are undergoing replication in mosquitoes [37]. Data from mosquitoes held at constant
293 temperatures supports these prior findings: d_N/d_S was generally near or above 1. In some cases,
294 (e.g. 28°C and 35°C) strong positive selection was detected within the E and NS1 coding
295 regions. Positive selection observed at 35°C seems likely to be due to virus adaption to some
296 component of the mosquito stress response such has heat shock protein [38, 39]. The
297 mechanisms that give rise to the signal of positive selection at 28°C are not clear but may be

298 due to a bottleneck that by chance resulted in a genome with one or more nonsynonymous
299 variants that rose in frequency due to this stochastic event rather than natural selection. The
300 strong purifying selection observed in mosquitoes held at diurnal temperatures is detectable
301 mainly in nonstructural coding sequences, and principally in NS5. This seems logical given the
302 role of NS5-encoded proteins in virus replication [40] and highlights the requirement for
303 replicase functionality across a wide temperature gradient. Indeed, our data suggest that
304 ZIKV NS5 is adapted to temperature variation rather than to any individual temperature.

305 Analysis of consensus sequences taken from different mosquito tissues allowed us to identify
306 the impacts of virus dissemination and physiological barriers on ZIKV sequences during
307 systemic infection. Generally, our data demonstrate a positive correlation between constant
308 temperature and nucleotide diversity (Fig 2E). As the virus disseminates into saliva, nucleotide
309 diversity increases both with temperature and in a stepwise manner as new tissue
310 compartments are infected. These findings indicate that at higher temperatures, more new
311 consensus variants are generated. The impact of diurnal temperatures differed between two
312 species, with most new consensus variants generated at diurnal temperatures by the less-
313 efficient vector *Ae. albopictus*. These observations demonstrate that temperature gradients and
314 fluctuations, and virus transmission by new, perhaps less efficient vector species, can drive the
315 emergence of new virus variants during mosquito infection, and are supported by analyses of
316 divergence that incorporate both intra- and interhost variation. Therefore, migration of
317 arboviruses such as ZIKV into new environments containing unexplored vectors represents an
318 opportunity for the emergence of new virus variants.

319 **Increased extrinsic incubation temperatures drive viral variant fixation in mosquitoes**

320 We identified 8 consensus mutations (5 non-synonymous and 3 synonymous) in multiple
321 mosquitoes during the course of this study. These all were present in the input population at low
322 frequencies (0.01- 0.35, Table 1) and rose in frequency during mosquito infection. Four

323 consensus changes were found in both *Aedes* species, and in mosquitoes held under most
324 temperature regimes. L330V E (Fig S1A) is within domain III of the envelope protein, which
325 plays a role in host cell receptor binding and entry [41]. W98G NS1 (Fig S1B) is a surface
326 exposed aromatic to aliphatic amino acid change on the wing section of NS1, which contributes
327 to cellular membrane association [42]. M220T NS1 (Fig S1C) replaces a sulfur containing side
328 group with a hydroxylic side group and is located on the loop surface the NS1 172-352
329 homodimer [43]. G83 NS5 (Fig S1D) is a synonymous mutation found in the middle of the
330 coding sequence for the NS5 methyltransferase domain active site. Moreover most of these
331 substitutions were not particularly conservative and may be of functional significance.
332 While none of these mutations increased significantly in frequency at 25°C, mosquito exposure
333 to 35°C or diurnal temperatures cause some of these mutations to rise in frequency,
334 sometimes in a species-dependent manner, again highlighting the temperature-dependence
335 of variant frequencies in our studies.
336 To assess the fitness implications of these and other mutations that were repeatedly detected in
337 mosquitoes, we engineered individual mutations into a ZIKV infectious clone and conducted *in*
338 *vivo* competition studies at 25° and 35°C. The most notable finding from these studies is that
339 higher temperatures tended to favor frequently detected mutations, which is consistent with our
340 data on variant frequencies, consensus level changes and the strength of purifying selection.
341 Accordingly, we conclude that the variants we examined are more likely to reach high frequency
342 at higher temperature.
343 The work presented here was designed to address the hypothesis that temperature determines
344 not only the efficiency with which mosquitoes transmit arboviruses (which has been well
345 established for decades) but that it also influences virus evolutionary dynamics. The lack of
346 quantitative data on how temperature effects arbovirus mutational diversity and selective forces
347 within mosquitoes is a critical shortcoming in the literature. Data presented here provides some
348 novel insights into this. The most significant findings reported here are related to how increases

349 in temperature increase the rate of fixation of novel variants in virus populations, both at the
350 population and consensus sequence levels. This suggests that as global temperatures rise, new
351 virus variants may emerge more rapidly. This observation requires validation using other virus-
352 vector pairs, but the implications are ominous and require further attention.
353 A second key finding is that diurnal temperatures impose heretofore undetected purifying
354 selection on virus populations as they pass through mosquitoes. This finding was not predicted,
355 but was consistent in both mosquito species examined. We suspect that this finding is related to
356 both (a) increased constraint imposed by the requirement that the virus replicase act efficiently
357 across a ten degree Celsius temperature range and (b) the inability of potentially temperature-
358 specific adaptive mutations to rise in frequency. Our data on individual mutations in various
359 mosquito tissues supports this. Moreover, this work collectively highlights the significance of
360 temperature changes on the evolutionary biology of the mosquito-virus interaction. It also
361 indicates that studies of arbovirus-vector interactions conducted using multiple temperatures,
362 including diurnal temperature cycles, may capture subtle yet significant evolutionary forces that
363 act on viruses during mosquito infection.

364 **Methods**

365 **Cells and Virus**

366 African Green Monkey kidney cells (Vero; ATCC CCL-81) were maintained at 37°C and 5% CO₂
367 in Dulbecco's modified Eagle's medium (DMEM) supplemented with 10% fetal bovine serum
368 (FBS) and 1% penicillin-streptomycin (Pen-Strep). Zika virus strain PRVABC59 (ZIKV-
369 PRVABC59; GenBank # KU501215) obtained from the Center for Disease Control and
370 Prevention branch in Fort Collins, CO was originally isolated from the sera of a patient returning
371 from travel to Puerto Rico in December 2015. The virus was isolated on Vero cells and a 4th
372 passage frozen at -80 was used for all *in vivo* and *in vitro* experiments. ZIKV-PRVABC59
373 infectious clone (ZIKV-PR-IC) served as a backbone for the reverse genetic platform developed

374 by our lab [44] to introduce all point mutations. ZIKV-REF was designed using the
375 aforementioned reverse genetic platform, incorporating 5 synonymous mutations amino acid
376 108-arginine and 109-serine of the prM protein coding sequence. The ZIKV-PR-IC sequence
377 nucleotides were changed from ZIKV-PR-IC 795-CGG TCG-800 to ZIKV-REF 795-AGA AGT-
378 200.

379 **Mosquitoes**

380 *Ae. aegypti* colonies for this study were established from individuals collected in Poza Rica,
381 Mexico [45] and used at F13-F18 generation. A lab adapted colony (greater than 50
382 generations) of *Ae. albopictus* were established from individuals collected in Florida, USA; the
383 colony was provided by the Centers for Diseases Control and Prevention (CDC-Fort Collins,
384 CO, USA) in 2010. Mosquitoes were reared and maintained at 27-28°C and 70-80% relative
385 humidity with a 12:12 L:D photoperiod. Water and sucrose were provided ad libitum.

386 **Infection of Aedes mosquitoes and sample collection**

387 Adult mosquitoes used for experiments were 3-7 days post-eclosion. Mosquitoes were provided
388 a bloodmeal containing calf blood mixed 1:1 with ZIKV-PRVABC59 (1E7 PFU/mL) using a water
389 jacketed glass membrane feeder. Engorged female mosquitoes were sorted into cartons and
390 housed at 25°C, 28°C, 32°C, 35°C at constant temperatures or alternating between 25°C -35°C
391 to simulate diurnal condition, with 70-80% relative humidity and 12:12 L:D photoperiod.
392 Mosquitoes were cold anesthetized in preparation for dissociations. Mosquito midguts,
393 legs/wings, and saliva from the first batch of mosquitoes were collected after 7- and 14-days
394 post-feed for NGS processing. Mosquito carcass, legs/wings and saliva from the second batch
395 of mosquitoes were collected at 3, 5, 7, 10, and 14 days post-feed for assessing systemic
396 infecting dynamics. Tissues represent infection (midgut), dissemination (legs), and transmission
397 (saliva). Tissues were removed using forceps cleaned with 70% ethanol between samples and

398 were homogenized in 200 μ l of mosquito diluent with a stainless-steel ball bearing using a
399 Retsch Mixer Mill 400 at 24 Hz for 45 seconds, as previously described [46]. Saliva was
400 collected by inserting mosquito mouthparts into capillary tubes containing mineral oil for 30 to 45
401 minutes. Saliva in oil was removed from the capillary tube by centrifugation into 100 μ l of
402 mosquito diluent for 5 minutes at $>20,000 \times g$. All samples were stored at -80°C until
403 manipulation.

404 **Plaque assay**

405 ZIKV stocks and infectious bloodmeal were quantified by plaque assay on Vero cell cultures
406 seeded in 12-well plates. Duplicate wells were infected with 0.2 ml aliquots from serial 10-fold
407 dilutions of virus stocks and infectious blood meals in media (DMEM supplemented with 1%
408 FBS and 1% penicillin/streptomycin), and virus was adsorbed for one hour by incubating at
409 37 °C in 5% CO₂. Following incubation, the inoculum was removed, and monolayers were
410 overlaid with tragacanth-EMEM overlay containing 1x EMEM, 5x L-glutamine, sodium
411 bicarbonate 3.75%, tragacanth 1.2%, gentamicin (25mg/ml), and Amphotericin B 40mL/L. Cells
412 were incubated at 37 °C in 5% CO₂ for four days for plaque development. Cell monolayers then
413 were stained with 1 mL of overlay containing a 20% ethanol and 0.1% crystal violet. Cells were
414 incubated at room temperature for 30-60 minutes and then gently washed and plaques were
415 counted. Plaque assays for 3,5,7,10 and 14 days post infection (dpi) mosquitoes were
416 performed similar to above with the following changes, 50 μ l of homogenized midgut and leg
417 tissues or 30 μ l of saliva samples were added to Vero cultures in 24-well plates (final volume of
418 200 μ l), and plaques were observed post processing.

419 **Viral RNA isolation**

420 Viral RNA was extracted from 50 μ l of either cell culture supernatant, homogenized mosquito
421 tissues, or saliva-containing solution using the Mag-Bind® Viral DNA/RNA 96 kit (Omega Bio-

422 Tek) on the KingFisher Flex Magnetic Particle processor (Thermo Fisher Scientific). Nucleic
423 acid extraction was performed as directed by the manufacturer and eluted in 50 μ l nuclease-free
424 water. Viral RNA was then quantified by qRT-PCR using the iTaqTM Universal Probes One-Step
425 Kit (BIO-RAD) according to manufacturer's protocol using a forward primer (5'-
426 CCGCTGCCAACACAAG-3'), reverse primer (5'- CCACTAACGTTCTTGCAGACAT-3'), and
427 FAM probe (5'- AGCCTACCTTGACAAGCAGTCAGACACTCAA-3') sequences [47].

428 **Generation of ZIKV mutant clones**

429 An infectious clone for ZIKV-PRVABC59 was used to generate mutants [44]. To engineer the
430 point mutations (Table 1) into the ZIKV genome, the corresponding single nucleic acid
431 substitution was introduced into the ZIKV-PR-IC using *in vivo* assembly cloning methods [48].
432 The infectious clone plasmids were linearized by restriction endonuclease digestion, PCR
433 purified, and ligated with T4 DNA ligase. From the assembled fragments, capped T7 RNA
434 transcripts were generated, and the resulting RNA was electroporated into Vero cells. Infectious
435 virus was harvested when 50-75% cytopathic effects were observed (5-8 days post
436 transfection). Viral supernatant was clarified by centrifugation and supplemented to a final
437 concentration of 20% fetal bovine serum and 10 mM HEPES prior to freezing and storage as
438 single use aliquots. Titer was measured by plaque assay on Vero cells. All stocks (both wildtype
439 and infectious clone-derived viruses) were sequenced via sanger sequencing to verify complete
440 genome sequence.

441 **Competition studies**

442 Competitive fitness was determined largely as described in previous studies [49, 50].
443 Competitions were conducted with orally infected *Ae. aegypti* (Poza Rica) mosquitoes. Three to
444 seven day old mosquitoes were offered a bloodmeal containing the 1:1 mixture of viruses
445 (ZIKV-REF and ZIKV-clone of interest) at a concentration of 1 million PFU/mL and bodies were

446 collected 14 days post blood feed. RNA was extracted as above, and amplicons were generated
447 via qRT-PCR using iTaq™ Universal SYBR® Green One-Step Kit (BIO-RAD) according to
448 manufacture protocol. A locked nucleic acid (LNA) forward primer was used to ensure amplicon
449 specificity. The forward LNA primer 5'-A+CTTGGGTTGTGTACGG-3' and reverse primer 5'-
450 GTTCCAAGACAACATCAACCCA-3' were used to generate amplicons for Quantitative Sanger
451 sequencing. Genotype fitness was analyzed using polySNP software [51] to measure the
452 proportion of the five synonymous variants present in the ZIKV-REF sequence allowing us to
453 compare the proportion of ZIKV-REF virus to competitor virus.

454 **Library preparation for next-generation sequencing**

455 Positive controls were generated in triplicate, each generated with 1 million genome equivalents
456 of a 100% ZIKV PRVABC59 viral stock, a mixture of 90% ZIKV PRVABC59 and 10% ZIKV
457 PA259359 (GenBank # KX156774.2), and a mixture of 99% ZIKV PRVABC59 and 1% ZIKV
458 PA259359. The negative control was water (no template control, or NTC). Controls and sample
459 RNA (10ul) was prepared for NGS using the Trio RNA-Seq Library Preparation Kit (NUGEN) per
460 manufacturer standard protocol. Final libraries were pooled by tissue type and analyzed for size
461 distribution using the Agilent High Sensitivity D1000 Screen Tape on the Agilent Tapestation
462 2200, final quantification was performed using the NEBNext® Library Quant Kit for Illumina®
463 (NEB) according to manufacturer's protocol. 150 nt paired-end reads were generated using the
464 Illumina HiSeq4000 at Genewiz.

465 **NGS processing and data analysis**

466 NGS data were analyzed using a workflow termed "RPG (RNA virus Population Genetics)
467 Workflow"; this workflow was generated using Snakemake [52] and workflow and related
468 documentation can be found at <https://bitbucket.org/murrieta/snakefile/src>. Briefly, Read 1
469 and Read 2 .fastq files from paired-end Illumina HiSeq 4000 data were trimmed for Illumina

470 adaptors and quality trimming of phred scores < 30 from the 3' and 5' read ends using cutadapt
471 [53]. The reads were then mapped to the ZIKV-PRVABC59 reference sequence (GenBank #
472 KU501215) using MOSAIK [54], similar to that previously described [55]. Picard [56], Genome
473 Analysis Toolkit (GATK) [57], and SAMtools [58] were used for variant calling preprocessing.
474 SNV's and inserts and deletions (INDELS) we called using LoFreq [59] with the --call-indels
475 command; otherwise, all settings were default. Consensus sequences were generated using the
476 .vcf files generated above and VCFtools [60]. NTC had less than 0.02% of reads mapping to
477 ZIKV and an average of < 8x coverage across the genome indicating little to no contamination,
478 sequencing bleed through, or index hopping (S1 Table). Only variants in the coding sequence
479 (nt position 108-10379), with 100x coverage or greater and a cut off of 0.01 frequency were used
480 for analysis to account for low coverage (reads per genome position) in the 3' and 5'
481 untranslated regions (S1 Table, Fig S2).

482 Data analysis was performed using custom Python and R code integrated into the RPG
483 Workflow. Using .vcf files generated by LoFreq and .depth files generated by GATK
484 DepthOfCoverage command, the workflow generates .csv files that provides sequencing
485 coverage across the CDS, Shannon entropy, richness, nucleotide diversity, d_N/d_S , and F_{ST}
486 (compared to input population) of a specified locus. Additionally, amino acid changes,
487 synonymous (S) and non-synonymous (NS) changes, and Shannon entropy are reported by
488 variant positions. The same scripts are called manually outside of the RPG Workflow to perform
489 the above analysis on specific protein coding regions or to compare divergence of populations
490 other than the input.

491 **Genetic diversity**

492 All genetic diversity calculations were incorporated into Python and R code located at
493 <https://bitbucket.org/murrieta/snakefile/src/master/scripts/>. In short, richness was calculated

494 by the sum of the intrahost SNV (iSNV) sites detected in the CDS in each population. Diversity
495 was calculated by the sum of the iSNV frequencies per coding sequence. Complexity was
496 calculated using Shannon entropy (S) which was calculated for each intrahost population (i)
497 using the iSNV frequency (p) at each nucleotide position (s):

498 (1)
$$S_{i,s} = -(p_s(\log_2 p_s) + (1 - p_s)\log_2(1 - p_s))$$

499 The mean S from all sites s is used to estimate the mutant spectra complexity. Divergence was
500 calculated using F_{ST} to estimate genetic divergence between two viral populations as described
501 previously [55]

502 **Selection**

503 Intrahost selection was estimated by the ratio of nonsynonymous (d_N) to synonymous (d_S) SNVs
504 per site (d_N/d_S) using the Jukes-Cantor formula as previously described [55], and incorporated
505 into custom Python code found at <https://bitbucket.org/murrieta/snakemake/src/master/scripts/>.
506 DnaSP software [61] was used to determine the number of nonsynonymous (7822.83) and
507 synonymous (2446.17) sites from the ancestral input ZIKV consensus sequence. When no
508 synonymous SNVs sites were present in replicates, d_N/d_S was set to 1, and no nonsynonymous
509 SNV's d_N/d_S was set to 0.

510 **Statistical analysis**

511 All analyses were performed using GraphPad Prism (version 7.04) and R. Fisher's exact test
512 were used to determine significant difference in virus titers and viral loads. All other tests were
513 done using Kruskal-Wallis with Dunn's correction unless otherwise noted.
514 To evaluate the relationship between external factors and the infection dynamics of ZIKV, we
515 examined the data with generalized linear models (Supplemental material). The predictors we

516 used include days post infection (days), temperature (scaled), species, and tissue type. We
517 evaluated the impact of these variables on consensus changes, vector competence, complexity,
518 nucleotide diversity and richness. We assumed that consensus changes and richness follow a
519 quasi-Poisson distribution, complexity and nucleotide diversity follow a linear distribution, and
520 assumed that dissemination efficiency and vector competence follow a binomial distribution. Our
521 original models follow the base structure

522 (2)
$$response \sim \exp [\beta_1(days) * \beta_2(temp)^2 * \beta_3(species) * \beta_4(tissue)]$$

523 Each model was reduced to a best fit structure using AIC values and/or a chi-square goodness
524 of fit test. The polynomial on temperature allows us to differentiate between the linear and
525 quadratic effect of temperature. Vector competence was evaluated with the following base
526 structure for each tissue response

527 (3)
$$response \sim \exp [\beta_1(days) * \beta_2(temp)^2 * \beta_3(species)]$$

528 **Data Availability**

529 Zika virus sequence data have been deposited in the NCBI Sequence Read Archive
530 (PRJNA659260). All other data supporting the findings given are available within the article and
531 supplementary information files, or from corresponding author upon request.

532 **Acknowledgments:**

533 The authors would like to acknowledge the CDC Arbovirus Reference Collection (CDC, Fort
534 Collins) for providing the ZIKV strain used in this study. Furthermore, we would like to
535 acknowledge Erin McDonald (CDC, Fort Collins) for providing the L330V-E and W98G-NS1
536 ZIKV plasmids and Irma Sanchez-Vargas (CSU) for providing the *Ae. albopictus* colony used in
537 this study.

538 **References**

539 1. Kuno G, Mackenzie JS, Junglen S, Hubalek Z, Plyusnin A, Gubler DJ. Vertebrate Reservoirs of
540 Arboviruses: Myth, Synonym of Amplifier, or Reality? *Viruses*. 2017;9(7). Epub 2017/07/14. doi:
541 10.3390/v9070185. PubMed PMID: 28703771; PubMed Central PMCID: PMC5537677.

542 2. Garmel GM. An Introduction to Clinical Emergency Medicine. 2nd ed2012.

543 3. Ryan SJ, Carlson CJ, Mordecai EA, Johnson LR. Global expansion and redistribution of Aedes-
544 borne virus transmission risk with climate change. *PLoS Negl Trop Dis*. 2019;13(3):e0007213. Epub
545 2019/03/29. doi: 10.1371/journal.pntd.0007213. PubMed PMID: 30921321; PubMed Central PMCID:
546 PMC56438455.

547 4. Hardy JL, Houk EJ, Kramer LD, Reeves WC. Intrinsic factors affecting vector competence of
548 mosquitoes for arboviruses. *Annual review of entomology*. 1983;28:229-62. doi:
549 10.1146/annurev.en.28.010183.001305. PubMed PMID: 6131642.

550 5. Chamberlain RW, Sudia WD. The effects of temperature upon the extrinsic incubation of eastern
551 equine encephalitis in mosquitoes. *American journal of hygiene*. 1955;62(3):295-305. PubMed PMID:
552 13268419.

553 6. Turell MJ, Rossi CA, Bailey CL. Effect of extrinsic incubation temperature on the ability of Aedes
554 taeniorhynchus and Culex pipiens to transmit Rift Valley fever virus. *Am J Trop Med Hyg*.
555 1985;34(6):1211-8. Epub 1985/11/01. doi: 10.4269/ajtmh.1985.34.1211. PubMed PMID: 3834803.

556 7. Lane WC, Dunn MD, Gardner CL, Lam LKM, Watson AM, Hartman AL, et al. The Efficacy of the
557 Interferon Alpha/Beta Response versus Arboviruses Is Temperature Dependent. *mBio*. 2018;9(2). Epub
558 2018/04/25. doi: 10.1128/mBio.00535-18. PubMed PMID: 29691338; PubMed Central PMCID:
559 PMC5915735.

560 8. Tesla B, Demakovskiy LR, Mordecai EA, Ryan SJ, Bonds MH, Ngonghala CN, et al. Temperature
561 drives Zika virus transmission: evidence from empirical and mathematical models. *Proc Biol Sci*.
562 2018;285(1884). Epub 2018/08/17. doi: 10.1098/rspb.2018.0795. PubMed PMID: 30111605; PubMed
563 Central PMCID: PMC5611177.

564 9. Winokur OC, Main BJ, Nicholson J, Barker CM. Impact of temperature on the extrinsic incubation
565 period of Zika virus in Aedes aegypti. *PLoS Negl Trop Dis*. 2020;14(3):e0008047. Epub 2020/03/19. doi:
566 10.1371/journal.pntd.0008047. PubMed PMID: 32187187; PubMed Central PMCID: PMC7105136.

567 10. Reisen WK, Fang Y, Martinez VM. Effects of temperature on the transmission of west nile virus
568 by Culex tarsalis (Diptera: Culicidae). *J Med Entomol*. 2006;43(2):309-17. Epub 2006/04/20. doi:
569 10.1603/0022-2585(2006)043[0309:EOTOTT]2.0.CO;2. PubMed PMID: 16619616.

570 11. Richards SL, Lord CC, Pesko K, Tabachnick WJ. Environmental and biological factors influencing
571 Culex pipiens quinquefasciatus Say (Diptera: Culicidae) vector competence for Saint Louis encephalitis
572 virus. *Am J Trop Med Hyg*. 2009;81(2):264-72. PubMed PMID: 19635881; PubMed Central PMCID:
573 PMC2808141.

574 12. Keyel AC, Elison Timm O, Backenson PB, Prussing C, Quinones S, McDonough KA, et al. Seasonal
575 temperatures and hydrological conditions improve the prediction of West Nile virus infection rates in
576 Culex mosquitoes and human case counts in New York and Connecticut. *PLoS One*.
577 2019;14(6):e0217854. Epub 2019/06/04. doi: 10.1371/journal.pone.0217854. PubMed PMID: 31158250;
578 PubMed Central PMCID: PMC6546252.

579 13. Kilpatrick AM, Meola MA, Moudy RM, Kramer LD. Temperature, viral genetics, and the
580 transmission of West Nile virus by Culex pipiens mosquitoes. *PLoS Pathog*. 2008;4(6):e1000092. doi:
581 10.1371/journal.ppat.1000092. PubMed PMID: 18584026; PubMed Central PMCID: PMC2430533.

582 14. Turell MJ. Effect of environmental temperature on the vector competence of Aedes
583 taeniorhynchus for Rift Valley fever and Venezuelan equine encephalitis viruses. *Am J Trop Med Hyg*.
584 1993;49(6):672-6. Epub 1993/12/01. doi: 10.4269/ajtmh.1993.49.672. PubMed PMID: 8279634.

585 15. Vogels CB, Fros JJ, Goertz GP, Pijlman GP, Koenraadt CJ. Vector competence of northern
586 European Culex pipiens biotypes and hybrids for West Nile virus is differentially affected by

587 temperature. *Parasit Vectors*. 2016;9(1):393. Epub 2016/07/09. doi: 10.1186/s13071-016-1677-0.
588 PubMed PMID: 27388451; PubMed Central PMCID: PMCPMC4937539.

589 16. Patz JA, Epstein PR, Burke TA, Balbus JM. Global climate change and emerging infectious
590 diseases. *Jama*. 1996;275(3):217-23. PubMed PMID: 8604175.

591 17. Garcia-Luna SM, Weger-Lucarelli J, Ruckert C, Murrieta RA, Young MC, Byas AD, et al. Variation
592 in competence for ZIKV transmission by *Aedes aegypti* and *Aedes albopictus* in Mexico. *PLoS Negl Trop*
593 *Dis*. 2018;12(7):e0006599. Epub 2018/07/03. doi: 10.1371/journal.pntd.0006599. PubMed PMID:
594 29965958; PubMed Central PMCID: PMCPMC6044546.

595 18. Weger-Lucarelli J, Ruckert C, Chotiwan N, Nguyen C, Garcia Luna SM, Fauver JR, et al. Vector
596 Competence of American Mosquitoes for Three Strains of Zika Virus. *PLoS Negl Trop Dis*.
597 2016;10(10):e0005101. doi: 10.1371/journal.pntd.0005101. PubMed PMID: 27783679; PubMed Central
598 PMCID: PMC5081193.

599 19. Gendernalik A, Weger-Lucarelli J, Garcia Luna SM, Fauver JR, Ruckert C, Murrieta RA, et al.
600 American *Aedes vexans* Mosquitoes are Competent Vectors of Zika Virus. *Am J Trop Med Hyg*.
601 2017;96(6):1338-40. Epub 2017/07/19. doi: 10.4269/ajtmh.16-0963. PubMed PMID: 28719283; PubMed
602 Central PMCID: PMCPMC5462567.

603 20. Kenney JL, Romo H, Duggal NK, Tzeng WP, Burkhalter KL, Brault AC, et al. Transmission
604 Incompetence of *Culex quinquefasciatus* and *Culex pipiens pipiens* from North America for Zika Virus.
605 *Am J Trop Med Hyg*. 2017;96(5):1235-40. Epub 2017/05/14. doi: 10.4269/ajtmh.16-0865. PubMed
606 PMID: 28500817; PubMed Central PMCID: PMCPMC5417222.

607 21. Paaijmans KP, Read AF, Thomas MB. Understanding the link between malaria risk and climate.
608 *Proc Natl Acad Sci U S A*. 2009;106(33):13844-9. Epub 2009/08/12. doi: 10.1073/pnas.0903423106.
609 PubMed PMID: 19666598; PubMed Central PMCID: PMCPMC2720408.

610 22. Carrington LB, Armijos MV, Lambrechts L, Scott TW. Fluctuations at a low mean temperature
611 accelerate dengue virus transmission by *Aedes aegypti*. *PLoS Negl Trop Dis*. 2013;7(4):e2190. Epub
612 2013/05/03. doi: 10.1371/journal.pntd.0002190. PubMed PMID: 23638208; PubMed Central PMCID:
613 PMCPMC3636080.

614 23. Carrington LB, Seifert SN, Willits NH, Lambrechts L, Scott TW. Large diurnal temperature
615 fluctuations negatively influence *Aedes aegypti* (Diptera: Culicidae) life-history traits. *J Med Entomol*.
616 2013;50(1):43-51. Epub 2013/02/23. doi: 10.1603/me11242. PubMed PMID: 23427651.

617 24. Lambrechts L, Paaijmans KP, Fansiri T, Carrington LB, Kramer LD, Thomas MB, et al. Impact of
618 daily temperature fluctuations on dengue virus transmission by *Aedes aegypti*. *Proc Natl Acad Sci U S A*.
619 2011;108(18):7460-5. Epub 2011/04/20. doi: 10.1073/pnas.1101377108. PubMed PMID: 21502510;
620 PubMed Central PMCID: PMCPMC3088608.

621 25. Alto BW, Wasik BR, Morales NM, Turner PE. Stochastic temperatures impede RNA virus
622 adaptation. *Evolution*. 2013;67(4):969-79. doi: 10.1111/evo.12034. PubMed PMID: 23550749.

623 26. McGee LW, Aitchison EW, Caudle SB, Morrison AJ, Zheng L, Yang W, et al. Payoffs, not tradeoffs,
624 in the adaptation of a virus to ostensibly conflicting selective pressures. *PLoS genetics*.
625 2014;10(10):e1004611. doi: 10.1371/journal.pgen.1004611. PubMed PMID: 25275498; PubMed Central
626 PMCID: PMC4183430.

627 27. Domingo E, Sabo D, Taniguchi T, Weissmann C. Nucleotide sequence heterogeneity of an RNA
628 phage population. *Cell*. 1978;13(4):735-44. PubMed PMID: 657273.

629 28. Holland J, Spindler K, Horodyski F, Grabau E, Nichol S, VandePol S. Rapid evolution of RNA
630 genomes. *Science*. 1982;215(4540):1577-85. PubMed PMID: 7041255.

631 29. Jerzak G, Bernard KA, Kramer LD, Ebel GD. Genetic variation in West Nile virus from naturally
632 infected mosquitoes and birds suggests quasispecies structure and strong purifying selection. *J Gen*
633 *Virol*. 2005;86(Pt 8):2175-83. doi: 10.1099/vir.0.81015-0. PubMed PMID: 16033965; PubMed Central
634 PMCID: PMC2440486.

635 30. Brackney DE, Brown IK, Nofchissey RA, Fitzpatrick KA, Ebel GD. Homogeneity of Powassan virus
636 populations in naturally infected *Ixodes scapularis*. *Virology*. 2010;402(2):366-71. doi:
637 10.1016/j.virol.2010.03.035. PubMed PMID: 20434750; PubMed Central PMCID: PMC2875267.

638 31. Ciota AT, Ehrbar DJ, Van Slyke GA, Payne AF, Willsey GG, Viscio RE, et al. Quantification of
639 intrahost bottlenecks of West Nile virus in *Culex pipiens* mosquitoes using an artificial mutant swarm.
640 *Infect Genet Evol*. 2012;12(3):557-64. doi: 10.1016/j.meegid.2012.01.022. PubMed PMID: 22326536;
641 PubMed Central PMCID: PMC3314143.

642 32. Ruiz-Jarabo CM, Arias A, Baranowski E, Escarmis C, Domingo E. Memory in viral quasispecies. *J
643 Virol*. 2000;74(8):3543-7. PubMed PMID: 10729128; PubMed Central PMCID: PMC111862.

644 33. Vignuzzi M, Stone JK, Arnold JJ, Cameron CE, Andino R. Quasispecies diversity determines
645 pathogenesis through cooperative interactions in a viral population. *Nature*. 2006;439(7074):344-8. doi:
646 10.1038/nature04388. PubMed PMID: 16327776; PubMed Central PMCID: PMC1569948.

647 34. Franz AW, Kantor AM, Passarelli AL, Clem RJ. Tissue Barriers to Arbovirus Infection in
648 Mosquitoes. *Viruses*. 2015;7(7):3741-67. Epub 2015/07/18. doi: 10.3390/v7072795. PubMed PMID:
649 26184281; PubMed Central PMCID: PMCPMC4517124.

650 35. Mordecai EA, Caldwell JM, Grossman MK, Lippi CA, Johnson LR, Neira M, et al. Thermal biology
651 of mosquito-borne disease. *Ecol Lett*. 2019;22(10):1690-708. Epub 2019/07/10. doi: 10.1111/ele.13335.
652 PubMed PMID: 31286630; PubMed Central PMCID: PMCPMC6744319.

653 36. Mordecai EA, Cohen JM, Evans MV, Gudapati P, Johnson LR, Lippi CA, et al. Detecting the impact
654 of temperature on transmission of Zika, dengue, and chikungunya using mechanistic models. *PLoS Negl
655 Trop Dis*. 2017;11(4):e0005568. Epub 2017/04/28. doi: 10.1371/journal.pntd.0005568. PubMed PMID:
656 28448507; PubMed Central PMCID: PMCPMC5423694.

657 37. Grubaugh ND, Ebel GD. Dynamics of West Nile virus evolution in mosquito vectors. *Curr Opin
658 Virol*. 2016;21:132-8. Epub 2016/10/28. doi: 10.1016/j.coviro.2016.09.007. PubMed PMID: 27788400;
659 PubMed Central PMCID: PMCPMC5384794.

660 38. Benoit JB, Lopez-Martinez G, Phillips ZP, Patrick KR, Denlinger DL. Heat shock proteins contribute
661 to mosquito dehydration tolerance. *J Insect Physiol*. 2010;56(2):151-6. Epub 2009/09/29. doi:
662 10.1016/j.jinsphys.2009.09.012. PubMed PMID: 19782687; PubMed Central PMCID: PMCPMC2861860.

663 39. Gross TL, Myles KM, Adelman ZN. Identification and characterization of heat shock 70 genes in
664 *Aedes aegypti* (Diptera: Culicidae). *J Med Entomol*. 2009;46(3):496-504. Epub 2009/06/06. doi:
665 10.1603/033.046.0313. PubMed PMID: 19496419; PubMed Central PMCID: PMCPMC2702248.

666 40. Brinton MA. Replication cycle and molecular biology of the West Nile virus. *Viruses*.
667 2013;6(1):13-53. Epub 2014/01/01. doi: 10.3390/v6010013. PubMed PMID: 24378320; PubMed Central
668 PMCID: PMCPMC3917430.

669 41. Crill WD, Roehrig JT. Monoclonal antibodies that bind to domain III of dengue virus E
670 glycoprotein are the most efficient blockers of virus adsorption to Vero cells. *J Virol*. 2001;75(16):7769-
671 73. Epub 2001/07/20. doi: 10.1128/JVI.75.16.7769-7773.2001. PubMed PMID: 11462053; PubMed
672 Central PMCID: PMCPMC115016.

673 42. Xu X, Song H, Qi J, Liu Y, Wang H, Su C, et al. Contribution of intertwined loop to membrane
674 association revealed by Zika virus full-length NS1 structure. *EMBO J*. 2016;35(20):2170-8. Epub
675 2016/11/01. doi: 10.15252/embj.201695290. PubMed PMID: 27578809; PubMed Central PMCID:
676 PMCPMC5069551.

677 43. Song H, Qi J, Haywood J, Shi Y, Gao GF. Zika virus NS1 structure reveals diversity of electrostatic
678 surfaces among flaviviruses. *Nat Struct Mol Biol*. 2016;23(5):456-8. Epub 2016/04/19. doi:
679 10.1038/nsmb.3213. PubMed PMID: 27088990.

680 44. Weger-Lucarelli J, Duggal NK, Bullard-Feibelman K, Veselinovic M, Romo H, Nguyen C, et al.
681 Development and Characterization of Recombinant Virus Generated from a New World Zika Virus
682 Infectious Clone. *J Virol*. 2016. doi: 10.1128/JVI.01765-16. PubMed PMID: 27795432.

683 45. Vera-Maloof FZ, Saavedra-Rodriguez K, Elizondo-Quiroga AE, Lozano-Fuentes S, Black IV WC.
684 Coevolution of the Ile1,016 and Cys1,534 Mutations in the Voltage Gated Sodium Channel Gene of
685 *Aedes aegypti* in Mexico. *PLoS Negl Trop Dis.* 2015;9(12):e0004263. Epub 2015/12/15. doi:
686 10.1371/journal.pntd.0004263. PubMed PMID: 26658798; PubMed Central PMCID: PMCPMC4684211.
687 46. Fauver JR, Pecher L, Schurich JA, Bolling BG, Calhoon M, Grubaugh ND, et al. Temporal and
688 Spatial Variability of Entomological Risk Indices for West Nile Virus Infection in Northern Colorado: 2006-
689 2013. *J Med Entomol.* 2016;53(2):425-34. Epub 2016/01/01. doi: 10.1093/jme/tjv234. PubMed PMID:
690 26718715; PubMed Central PMCID: PMCPMC5778898.
691 47. Lanciotti RS, Kosoy OL, Laven JJ, Velez JO, Lambert AJ, Johnson AJ, et al. Genetic and serologic
692 properties of Zika virus associated with an epidemic, Yap State, Micronesia, 2007. *Emerg Infect Dis.*
693 2008;14(8):1232-9. Epub 2008/08/06. doi: 10.3201/eid1408.080287. PubMed PMID: 18680646; PubMed
694 Central PMCID: PMCPMC2600394.
695 48. Garcia-Nafria J, Watson JF, Greger IH. IVA cloning: A single-tube universal cloning system
696 exploiting bacterial In Vivo Assembly. *Sci Rep.* 2016;6:27459. Epub 2016/06/07. doi: 10.1038/srep27459.
697 PubMed PMID: 27264908; PubMed Central PMCID: PMCPMC4893743.
698 49. Deardorff ER, Fitzpatrick KA, Jerzak GV, Shi PY, Kramer LD, Ebel GD. West Nile virus experimental
699 evolution in vivo and the trade-off hypothesis. *PLoS Pathog.* 2011;7(11):e1002335. Epub 2011/11/22.
700 doi: 10.1371/journal.ppat.1002335. PubMed PMID: 22102808; PubMed Central PMCID:
701 PMCPMC3213084.
702 50. Grubaugh ND, Smith DR, Brackney DE, Bosco-Lauth AM, Fauver JR, Campbell CL, et al.
703 Experimental evolution of an RNA virus in wild birds: evidence for host-dependent impacts on
704 population structure and competitive fitness. *PLoS Pathog.* 2015;11(5):e1004874. Epub 2015/05/21. doi:
705 10.1371/journal.ppat.1004874. PubMed PMID: 25993022; PubMed Central PMCID: PMCPMC4439088.
706 51. Hall GS, Little DP. Relative quantitation of virus population size in mixed genotype infections
707 using sequencing chromatograms. *Journal of virological methods.* 2007;146(1-2):22-8. doi:
708 10.1016/j.jviromet.2007.05.029. PubMed PMID: 17640742; PubMed Central PMCID: PMC2246048.
709 52. Koster J, Rahmann S. Snakemake-a scalable bioinformatics workflow engine. *Bioinformatics.*
710 2018;34(20):3600. Epub 2018/05/23. doi: 10.1093/bioinformatics/bty350. PubMed PMID: 29788404.
711 53. Martin M. Cutadapt Removes Adapter Sequences From High-Throughput Sequencing Reads.
712 *EMBnetjournal.* 17(1). doi: <https://doi.org/10.14806/ej.17.1.200>.
713 54. Lee WP, Stromberg MP, Ward A, Stewart C, Garrison EP, Marth GT. MOSAIK: a hash-based
714 algorithm for accurate next-generation sequencing short-read mapping. *PLoS One.* 2014;9(3):e90581.
715 doi: 10.1371/journal.pone.0090581. PubMed PMID: 24599324; PubMed Central PMCID: PMC3944147.
716 55. Grubaugh ND, Fauver JR, Ruckert C, Weger-Lucarelli J, Garcia-Luna S, Murrieta RA, et al.
717 Mosquitoes Transmit Unique West Nile Virus Populations during Each Feeding Episode. *Cell Rep.*
718 2017;19(4):709-18. Epub 2017/04/27. doi: 10.1016/j.celrep.2017.03.076. PubMed PMID: 28445723;
719 PubMed Central PMCID: PMCPMC5465957.
720 56. Picard GitHub: Broad Institute; [6/21/2020]. Available from:
721 <https://broadinstitute.github.io/picard/>.
722 57. Van der Auwera GA, Carneiro MO, Hartl C, Poplin R, Del Angel G, Levy-Moonshine A, et al. From
723 FastQ data to high confidence variant calls: the Genome Analysis Toolkit best practices pipeline. *Curr
724 Protoc Bioinformatics.* 2013;43:11 0 1-0 33. Epub 2014/11/29. doi: 10.1002/0471250953.bi1110s43.
725 PubMed PMID: 25431634; PubMed Central PMCID: PMCPMC4243306.
726 58. Li H, Handsaker B, Wysoker A, Fennell T, Ruan J, Homer N, et al. The Sequence Alignment/Map
727 format and SAMtools. *Bioinformatics.* 2009;25(16):2078-9. doi: 10.1093/bioinformatics/btp352.
728 PubMed PMID: 19505943; PubMed Central PMCID: PMC2723002.
729 59. Wilm A, Aw PP, Bertrand D, Yeo GH, Ong SH, Wong CH, et al. LoFreq: a sequence-quality aware,
730 ultra-sensitive variant caller for uncovering cell-population heterogeneity from high-throughput

731 sequencing datasets. *Nucleic Acids Res.* 2012;40(22):11189-201. doi: 10.1093/nar/gks918. PubMed
732 PMID: 23066108; PubMed Central PMCID: PMC3526318.
733 60. Danecek P, Auton A, Abecasis G, Albers CA, Banks E, DePristo MA, et al. The variant call format
734 and VCFtools. *Bioinformatics*. 2011;27(15):2156-8. Epub 2011/06/10. doi:
735 10.1093/bioinformatics/btr330. PubMed PMID: 21653522; PubMed Central PMCID: PMCPMC3137218.
736 61. Librado P, Rozas J. DnaSP v5: a software for comprehensive analysis of DNA polymorphism data.
737 *Bioinformatics*. 2009;25(11):1451-2. Epub 2009/04/07. doi: 10.1093/bioinformatics/btp187. PubMed
738 PMID: 19346325.

739